

Light-induced amphiphilic surfaces

The ability to control the surface wettability of solid substrates is important in many situations. Here we report the photogeneration of a highly amphiphilic (both hydrophilic and oleophilic) titanium dioxide surface. The unique character of this surface is ascribed to the microstructured composition of hydrophilic and oleophilic phases, produced by ultraviolet irradiation. The result is a TiO_2 -coated glass which is antifogging and self-cleaning.

We prepared a thin TiO_2 polycrystalline film from anatase sol on a glass substrate, which was annealed at 773 K. The film showed a water-contact angle of $72^\circ \pm 1^\circ$ before ultraviolet irradiation (Fig. 1a). After irradiation, water droplets spread out on the film, resulting in a contact angle of $0^\circ \pm 1^\circ$ (Fig. 1b). This change in wettability was clearer when a TiO_2 -coated glass was exposed to water vapour. Without ultraviolet irradiation the glass fogged (Fig. 1c), but on irradiation the glass became transparent (Fig. 1d), a remarkable antifogging effect.

We also measured the contact angle using oily liquids (such as glycerol trioleate and hexadecane). We found distinct contact angles for the TiO_2 film under normal conditions, but all the liquids spread across the surface on ultraviolet irradiation, with contact angles of $0^\circ \pm 1^\circ$. Irradiation created a surface that was highly hydrophilic and highly oleophilic. We observed the wettability change on both anatase and rutile TiO_2 surfaces of polycrystals or single crystals, independent of their photocatalytic activities. Even after storage in the dark for a few days, the high amphiphilicity of the TiO_2 surface was maintained. A longer storage period induced a gradual increase in the water-contact angle, revealing a surface wettability trend towards hydrophobicity. However, high amphiphilicity was repeatedly regenerated by ultraviolet irradiation.

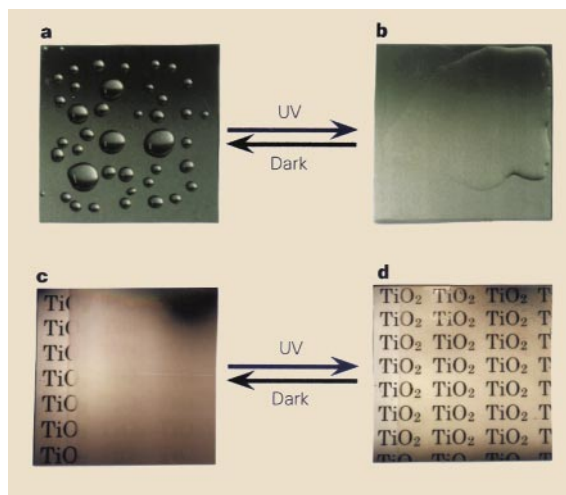
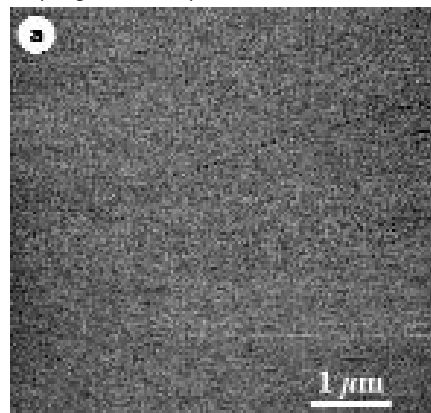


Figure 1 **a**, A hydrophobic surface before ultraviolet irradiation. **b**, A highly hydrophilic surface on ultraviolet irradiation. **c**, Exposure of a hydrophobic TiO_2 -coated glass to water vapour. The formation of fog (small water droplets) hindered the view of the text on paper placed behind the glass. **d**, Creation by ultraviolet irradiation of an antifogging surface. The high hydrophilicity prevents the formation of water droplets, making the text clearly visible.

The contact angle gives information about the macroscopic surface wettability. To gain information about surface wettability at a microscopic level we used friction force microscopy (FFM)¹. A rutile TiO_2 (110) single crystal was used to make these measurements because of its flat surface, a requirement for FFM. Before ultraviolet irradiation (Fig. 2a) we observed no difference in contrast, indicating microscopically homogeneous wettability. After irradiation, (Fig. 2b) hydrophilic (bright) and oleophilic (dark) areas of size 30–80 nm were clearly seen. Higher resolution images (Fig. 2b inset) show hydrophilic domains with regular rectangular shapes, aligned along the [001] direction of the (110) crystal surface, irrespective of the scanning direction. A gradual reversion to a lack of contrast was observed during the storage of the film in the dark. We conclude that the nanoscale separation between the hydrophilic and the oleophilic phases accounts for the highly amphiphilic character of the TiO_2 surface.

In combination with Fourier transform

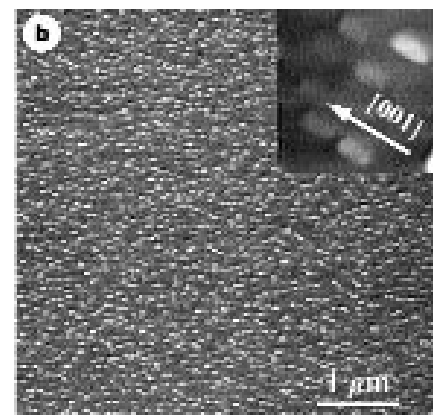


Figure 2 FFM images of a rutile TiO_2 (110) single crystal surface. **a**, A $5 \times 5 \mu\text{m}^2$ image before ultraviolet irradiation. **b**, The same surface after irradiation. Inset, topographic image ($245 \times 245 \text{ nm}$) acquired by rotating the sample stage through 45° to the large-scale image. The tip of the Si_3N_4 cantilever is hydrophilic, so hydrophilic areas are bright and hydrophobic areas are dark.

infrared spectroscopy and X-ray photoelectron spectroscopy studies, we propose the following model. Ultraviolet irradiation may create surface oxygen vacancies at bridging sites, resulting in the conversion of relevant Ti^{4+} sites to Ti^{3+} sites² which are favourable for dissociative water adsorption^{3,4}. These defects presumably influence the affinity to chemisorbed water of their surrounding sites, forming hydrophilic domains, whereas the rest of the surface remains oleophilic, as seen by FFM (Fig. 2b). The rectangular hydrophilic domains are areas where dissociative water is adsorbed, associated with oxygen vacancies that are preferentially photogenerated along the [001] direction of the (110) plane; the same direction in which oxygen bridging sites align⁵. Because a liquid droplet is substantially larger than the hydrophilic (or oleophilic) domain, it instantaneously spreads on such a surface, thereby resembling a two-dimensional capillary phenomenon. Microscopically, the hydrophilic and oleophilic areas are distinguishable, but macroscopically, the TiO_2 surface exhibits high amphiphilicity. On long-term storage in the dark, the chemisorbed hydroxyl groups are replaced with oxygen from the air³.

Such highly amphiphilic surfaces have many practical applications. Besides the antifogging effect (Fig. 1d), they are self-cleaning. Various substrates coated with TiO_2 films, regardless of their photocatalytic activities, showed obviously cleaner surfaces than those without TiO_2 coating after being hung outdoors for six months. Ultraviolet irradiation from sunlight is sufficient to maintain the amphiphilic surface, so that hydrophilic or oleophilic contaminants on the surfaces are easily removed by rain. This unique amphiphilic surface should be superior to a monohydrophilic or monoleophilic surface. The present system is independent of conventional photocatalytic reactions⁶, but the combination of these

two surface characters give TiO₂ materials a promising future.

Rong Wang, Kazuhito Hashimoto
Akira Fujishima

Department of Applied Chemistry,
Faculty of Engineering, University of Tokyo,
7-3-1 Hongo, Bunkyo-ku, Tokyo 113, Japan
e-mail: akira-fu@chem.t.u-tokyo.ac.jp

Makoto Chikuni, Eiichi Kojima
Atsushi Kitamura, Mitsuhide Shimohigoshi
Toshiya Watanabe

Research and Development Centre,
TOTO Ltd, 2-8-1, Honson Chigasaki-shi,
Kanagawa 253, Japan

1. Wilbur, J. L., Biebuyck, H. A., MacDonald, J. C. & Whitesides, G. M. *Langmuir* **11**, 825–831 (1995).
2. Shultz, A. N. *et al. Surface Sci.* **339**, 114–124 (1995).
3. Hugenschmidt, M. B., Gamble, L. & Campbell, C. T. *Surface Sci.* **302**, 329–340 (1994).
4. Henderson, M. A. *Surface Sci.* **355**, 151–166 (1996).
5. Murray, P. W., Condon, N. G. & Thornton, G. *Phys. Rev. B* **51**, 10989–10997 (1995).
6. Fujishima, A. & Honda, K. *Nature* **238**, 37–38 (1972).

S-nitrosylation regulates apoptosis

Nitric oxide (NO) modulates the biological activity of proteins by direct interactions with their iron centres. It can also S-nitrosylate cysteines to form S-nitrosothiols. Such reactions affect the activity of membrane-bound, cytosolic and nuclear proteins including the NMDA receptor¹, haemoglobin² and transcription factors such as NF- κ B³ and OxyR. NO is potentially toxic, inducing both apoptosis and necrosis. Here we show that NO-mediated S-nitrosylation of the cysteine-containing enzymes that mediate apoptosis (caspases and tissue-transglutaminase, tTG) regulates the balance between apoptosis and necrosis.

Apoptosis is triggered by caspases⁴ cleaving substrates such as poly(ADP ribose)-polymerase (PARP)⁵, and by tTG crosslinking of proteins⁶. We studied the effects of NO donors on cell death, PARP proteolysis and tTG activity. At 1 mM concentration, S-nitroso-N-acetylpenicillamine (SNAP) releases 60 nM free NO (ref. 3), therefore millimolar concentrations of pharmacological NO donors are needed to produce low micromolar concentrations of free NO in cells.

SNAP blocks apoptotic death in Jurkat T cells exposed to anti-CD95 (APO-1, Fas) antibody in a dose-dependent manner, as shown by FACS analysis (Fig. 1a), Hoechst 33342 staining and DNA laddering (not shown). The reduction of apoptosis was detectable after 3 h and significant after 6 h ($P < 0.001$).

Conversely, increasing concentrations of SNAP progressively increased necrotic cell death, as shown by trypan blue uptake (Fig.

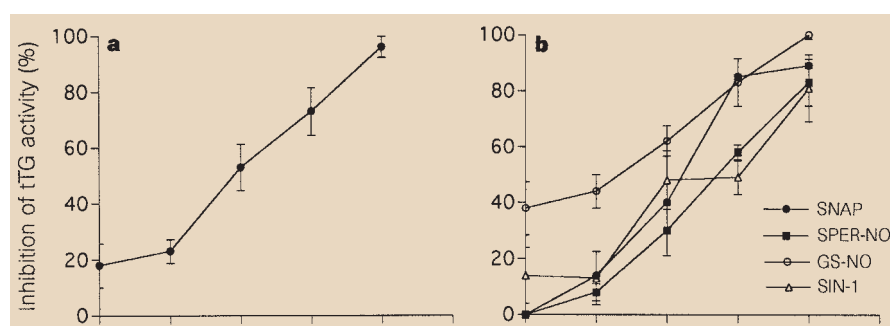
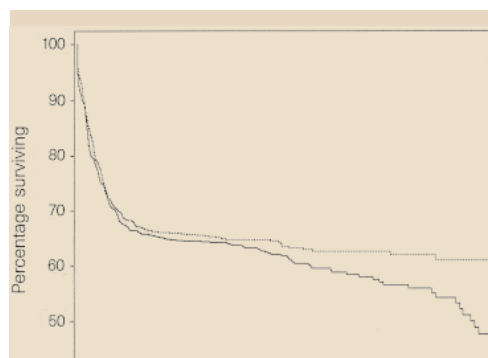


Figure 1 Mean dose- and time-dependent effect of SNAP on cell death assessed by: **a**, flow cytometry using propidium iodide⁶; and **b**, trypan blue uptake. Cells were exposed to SNAP (0.1–10 mM) alone or with 1 μ g ml⁻¹ anti-CD95 antibody and evaluated after 6 h. **c**, Inhibition of anti-CD95-induced proteolytic cleavage of PARP by SNAP. Cells were untreated (lane 1), incubated with SNAP (2–5) or 1 μ g ml⁻¹ anti-CD95 antibody (6–9) and with the NO donor (7–9) for 90 min. Extracts were analysed by western blotting using the monoclonal anti-PARP antibody C-2-10.



1b) and electron microscopy (not shown). Six hours after CD95 ligation, lactate dehydrogenase release increased by 10, 37, 45 and 180 IU l⁻¹ using 0, 0.1, 1.0 and 10 mM SNAP, respectively (baseline activity was 79 IU l⁻¹). Similar apoptosis/necrosis regulation was obtained by application of SNAP to Jurkat cells exposed to 30 μ M C6-ceramide (not shown).

SNAP (Fig. 1c) or GS-NO (S-nitroso-glutathione; not shown) inhibited CD95-triggered digestion of PARP by caspase-3 in a dose-dependent manner. This precedes the shift from apoptosis to necrosis triggered by CD95 ligation (90 min as opposed to 6 h). SNAP also inhibited the activity of purified tTG (Fig. 2a). This time-independent inhibition was prevented by NO scavengers. In the absence of D/L-dithiothreitol (DTT) the baseline activity of tTG was reduced from 1,200 \pm 160 to 41 \pm 6 nmol [³H]putrescine

per h per mg of protein, and significantly more NO was required to produce the same level of inhibition. DTT reduces the cysteine in the active site of tTG, activating the enzyme. The strong shift of the dose-response curve in the absence of DTT indicates that NO might react with this same cysteine.

Molecular modelling shows that nine of the 20 cysteines in tTG are close to the surface. NO reacts with one of the three titratable -SH groups: in fact, only two residues were detectable after exposure to 1 mM SNAP or 0.1 mM GS-NO. Similar results have been found for caspase-3 (ref. 7). Moreover, 1 mM spermine-NO eliminated two of the three titratable -SH groups, suggesting that free spermine, a natural tTG-substrate, binds to the substrate site and that this differs from the NO-bound active site.

Jurkat cells express little tTG, which is not required in CD95-induced apoptosis,

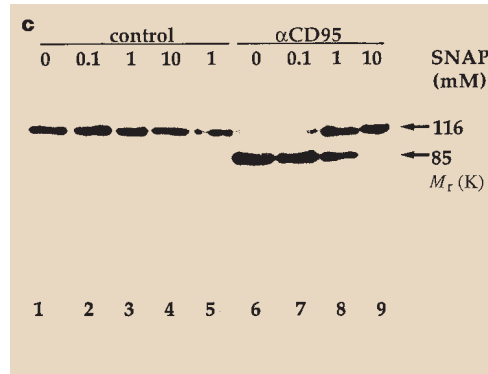


Figure 2 a, Effect of SNAP on purified tTG activity. SNAP was added to the enzyme preparation just before initiating the reaction with [³H]putrescine and *N,N*'-dimethylcasein. Purified tTG (86 nM) was incubated with 30 mM DTT for 20 min (ref. 6). Means of three experiments. **b**, Inhibition of tTG activity in SK-N-BE(2) cell extracts by increasing concentrations of the NO donors SNAP, spermine-NO, GS-NO or 3-morpholinosydnonimine (SIN-1). Extracts were exposed to donors immediately before the assay and incubated with 30 mM DTT for 20 min. Baseline activity was 215 \pm 24 and 161 \pm 18 pmol [³H]putrescine incorporated into *N,N*'-dimethylcasein per h per mg protein in the presence and absence of DTT, respectively. Means of three experiments.